An improved calculation of Coriolis terms on the C grid

Srdjan Dobricic[*]

Istituto Nazionale di Geofisica e Vulcanologia

Bologna, Italy

February 17, 2006

[*]dobricic@bo.ingv.it

Abstract

The central differencing grid with fully staggered velocity components (C grid) is widely used in primitive equations oceanographic models despite potential problems in simulating baroclinic inertia-gravity and Rossby waves that can arise due to the averaging of velocity components in the Coriolis terms. This note proposes a new averaging of the velocity components in order to calculate the Coriolis terms on the C grid. The averaging weights are calculated from the minimum of a suitably defined cost function which optimally minimizes the error in the inertial part of frequencies of inertia-gravity waves and maintains the second order accuracy of the computations. The theoretical analysis of wave frequency diagrams shows that the new scheme results in more accurate frequencies of long inertia-gravity and Rossby waves, especially when the Rossby radius of deformation is not resolved well by the grid resolution.

1. Introduction

The central differencing grid with fully staggered velocity components (C grid) is widely used in primitive equations oceanographic models (e.g. Haidvogel and Beckmann 1999). Arakawa and Lamb (1977) computed the frequencies of inertia-gravity waves for different finite differencing grids and found that C and B grids with the staggered height and velocity vectors components were giving satisfactory results for the geostrophic adjustment. The C grid was superior in simulating the gravity waves frequency, but it was less accurate in simulating the frequency of inertial waves, because the fully staggered position of velocity points (Figure 1) requires the averaging in order to compute the Coriolis term.

On the C grid the frequency of inertial waves, which in the analytical solution should be constant for all wavelengths, is correct only for the longest wave and monotonically decreases becoming equal to zero for the shortest wave. For a relatively large Rossby radius of deformation this problem is practically insignificant, because the frequency of gravity waves dominates the solution. However, in the ocean the first baroclinic Rossby radius of deformation is of order of only 10km in mid-latitudes, and becomes proportionally smaller for higher order baroclinic modes. When the Rossby radius of deformation is relatively small, the accuracy of the simulation of inertia-gravity waves may become sensitive to the accuracy of

the calculation of their inertial parts (e.g. Mesinger and Arakawa 1976). Furthermore, Wajsowicz (1986) showed that in this case the C grid also does not simulate accurately the frequency of Rossby waves.

Several methods were proposed to reduce or remove the effects of the C grid error in the calculation of the Coriolis terms in oceanographic models. Smith et al. (1990) applied the ”divergence damping” in the velocity field, but the *a posteriori* filtering of the small scales only reduces the effects of the error and can also remove an important part of the correct solution. Alternatively, Adcroft et al. (1999) combined C and D grids and calculated the Coriolis terms without the averaging, but the introduction of the D grid points required the use of 5 prognostic equations. The solution contained computational frequencies which were attenuated with a filter dependent on the time integration scheme and the time step length. Nechaev and Yaremchuk (2004) calculated Coriolis terms on the C grid without averaging using 4 independent prognostic equations for each velocity component. However, the use of 9 prognostic equations resulted in significantly longer computations and gives computational modes. Nechaev and Yaremchuk (2004) also proposed a computationally more efficient application of the same method with 3 prognostic equations. The resulting scheme does not change inertial frequencies on the C grid, but when used with the implicit time differencing, it selectively

damps short wave frequencies with the efficiency which depends on the length of the model time step.

In this note we will keep the standard distribution of the points on the C grid and will not try to reduce the effects of the averaging on the short scale noise. Instead, we will construct the averaging of the velocity components in the Coriolis terms in a way to optimally minimize the error in the frequency of the inertial oscillations. Section 2 will present the method to determine the optimal averaging. The theoretical improvements in the simulation of frequencies of inertia-gravity and Rossby waves will be shown in Section 3. In Section 4 a numerical experiment will demonstrate the impact of the improved averaging, and Section 5 will give conclusions.

2. Optimal averaging in Coriolis terms

The frequency of inertia-gravity waves follows from the solution of the linearized shallow water equations (e.g. Arakawa and Lamb 1977):

$$\frac{\partial u}{\partial t} - fv + g\frac{\partial h}{\partial x} = 0 \tag{1}$$

$$\frac{\partial v}{\partial t} + fu + g\frac{\partial h}{\partial y} = 0 \tag{2}$$

$$\frac{\partial h}{\partial t} + H\left(\frac{\partial u}{\partial x} + \frac{\partial v}{\partial x}\right) = 0 \tag{3}$$

where u and v are velocity components, h is the surface elevation displacement, g is the gravity acceleration, H the water depth (or the equivalent depth for baroclinic modes), and f is the Coriolis parameter which will be assumed constant in the derivation of inertia-gravity waves. The substitution of solutions in the form of waves

$$\begin{bmatrix} u \\ v \\ h \end{bmatrix} = \begin{bmatrix} u_0 \\ v_0 \\ h_0 \end{bmatrix} e^{i(kx+ly-\nu t)},$$

in addition to the geostrophic mode, gives the frequency of inertia-gravity waves:

$$\left(\frac{\nu}{f}\right)^2 = 1 + \lambda^2(k^2 + l^2), \tag{4}$$

where $\lambda = \sqrt{gH}/f$ is the Rossby radius of deformation.

[Figure 1 about here.]

On the C grid the finite differencing approximation of equations (1-2) (Arakawa and Lamb 1977) gives:

$$\frac{\partial u}{\partial t} - f\overline{v}^{xy} + g\delta_x h = 0 \tag{5}$$

$$\frac{\partial v}{\partial t} + f\overline{u}^{xy} + g\delta_y h = 0 \tag{6}$$

$$\frac{\partial h}{\partial t} + H\Big(\delta_x u + \delta_y v\Big) = 0 \tag{7}$$

Only the spatial differencing is substituted by the finite differencing, because the temporal differencing is not relevant for the optimal averaging. The substitution of wave solutions like (4) gives the approximation of the frequency of inertia-gravity waves on the C grid:

$$\left(\frac{\nu}{f}\right)^2 = cos^2\frac{X}{2}cos^2\frac{Y}{2} + 4\frac{\lambda^2}{d^2}\Big(sin^2\frac{X}{2} + sin^2\frac{Y}{2}\Big), \tag{8}$$

where $X = kd$, $Y = ld$, and d is the grid resolution assumed to be equal in x and y directions in order to simplify the presentation. In the analytical solution the first term on the right side of equation (4) is equal to 1 for all frequencies, while on the C grid (equation 8) it is $cos^2(X/2)cos^2(Y/2)$. Figure 2 shows that it is equal to 1 only for the longest wavelength and monotonically decreases to zero with the increasing wave number.

Now we will try to construct the averaging of the velocity in the Coriolis terms in equations (5) and (6) in a way to improve the simulated frequency. For simplicity we can first evaluate only the averaging in the i direction for the velocity

component v (see Figure 1). In the point corresponding to the i, with the standard averaging on the C grid in the direction i, $\overline{v}_i^*$ is calculated from nearest v points:

$$\overline{v}_i^* = \frac{v_{i-1/2} + v_{i+1/2}}{2}. \tag{9}$$

The Taylor expansion gives the truncation error of the averaging:

$$\epsilon^* = \frac{1}{8}\frac{\partial^2 v}{\partial x^2}d^2 + O(d^4). \tag{10}$$

The approximation has second other accuracy. However, there exists other second order accurate approximations. For example, if instead of the two nearest v points we average from the next pair of nearest v points along the i direction we get:

$$\overline{v}_i^{**} = \frac{v_{i-3/2} + v_{i+3/2}}{2}. \tag{11}$$

The Taylor expansion gives:

$$\epsilon^{**} = \frac{9}{8}\frac{\partial^2 v}{\partial x^2}d^2 + O(d^4). \tag{12}$$

The approximation still has second order accuracy, but now the error is 9 times larger. It is well known (e.g. Mesinger and Arakawa 1976) that equations (9) and (11) can be combined in a way to cancel the first terms on the right sides of (10) and (12) forming a fourth order accurate approximation. It can be easily verified that a fourth order averaging approximation from equations (9) and (11) is:

$$\overline{v}_i^{4th} = \frac{9}{8}\overline{v}_i^{*} - \frac{1}{8}\overline{v}_i^{**}. \tag{13}$$

[Figure 2 about here.]

However, instead of searching for a scheme with a smaller truncation error, we could look for an optimal solution that minimizes the error in the frequency of inertial oscillations without the condition for the improvement of the second order of accuracy. The general form of the solution will be:

$$\overline{v}_i^{o} = \alpha\overline{v}_i^{*} + (1-\alpha)\overline{v}_i^{**}, \tag{14}$$

The coefficient α will be determined from the minimum of the following cost function J:

$$J = \int_0^{\pi}\int_0^{\pi} w(\mu - 1)^2 dX dY, \tag{15}$$

where $w = w(X, Y)$ is a suitably defined weighting function and

$$\mu = \left[\alpha cos\frac{X}{2} + (1-\alpha)cos\frac{3X}{2}\right]\left[\alpha cos\frac{Y}{2} + (1-\alpha)cos\frac{3Y}{2}\right]. \qquad (16)$$

The function μ is the form of inertial part of the frequencies of inertia-gravity waves when the averaging from equation (14) is applied in directions x and y.

The solution will depend on the definition of w. We will show solutions corresponding to 3 definitions:

1) Constant w with equal weights for all waves.

2) Constant w for $X, Y < \pi/2$, and zero elsewhere. This form of w finds α which optimally minimizes the frequency error only for longer waves (with wavelengths greater than 4d).

3) Infinitely large w when $\mu > 1$, and constant w elsewhere. This solution requires that the optimal frequency of inertial waves is never larger than the analytical one.

The numerically found minimum of J corresponds to: 1) $\alpha = 1.33$, 2) $\alpha = 1.17$ and 3) $\alpha = 1.125$. It is interesting that the solution 3 is identical to the fourth order accurate averaging. It should be noticed that with some definitions of w it is also possible to find the minimum of J analytically, but we prefer the

numerical solution, because it can be easily recalculated for any w. Figure 2 shows the frequency of inertial waves corresponding to these values of α when $Y = 0$ and $Y = \pi/2$. All three solutions give significantly more accurate inertial waves frequencies than the standard second order accurate solution. However, the frequency simulated by the solution 1 overshoots the analytical solution in a broad part of the spectrum, and although it improves the solution for short waves more than any other scheme, its frequency is not improved for long waves. On the other hand, the frequency obtained by the solution 2 only slightly overshoots the analytical solution (the maximum is 1.033) and it is always closer to the analytical solution than the solution 3.

After also considering frequency solutions for many other definitions of w (not shown), we have decided to subjectively choose the solution 2 ($\alpha = 1.17$) as the most optimal one. The major reason for this choice is that it most accurately simulates the frequencies of long waves (waves longer than 4d). We can assume that long waves are the most important for the simulation of the geostrophic adjustment, and in numerical models short waves are anyway strongly damped by the horizontal viscosity. It gives the optimal averaging in the direction i:

$$\overline{v}_i^o = 1.17\overline{v}_i^*. - 0.17\overline{v}_i^{**}, \tag{17}$$

with the truncation error:

$$\epsilon^o = -\frac{0.36}{8}\frac{\partial^2 v}{\partial x^2}d^2 + O(d^4). \tag{18}$$

It is still second order accurate and its truncation error is slightly lower than in the standard averaging scheme.

In order to test the sensitivity of the result to the formulation of the function which has to be minimized within the cost function, another set of sensitivity calculations was performed with the definition $w(\mu^2 - 1)^2$. This could be a more natural choice because it better corresponds to the quadratic form of the equation (2). The results corresponding to the 3 formulations of w were: 1) $\alpha = 1.265$, 2) $\alpha = 1.17$ and 3) $\alpha = 1.125$. Therefore, for long waves it appears that this definition gives the same optimal solution $\alpha = 1.17$. In the appendix it is shown that the optimal averaging conserves the energy when calculated in the following flux form:

$$\frac{\partial u}{\partial t} = \frac{1}{\Delta x}\overline{f\overline{V}^{ox}}^{oy} + \ldots, \tag{19}$$

$$\frac{\partial v}{\partial t} = -\frac{1}{\Delta y}\overline{f\overline{U}^{oy}}^{ox} + \ldots, \tag{20}$$

where $U = u\Delta y$ and $V = v\Delta x$, and Δx and Δy are variable distances between grid points.

[Figure 3 about here.]

3. Properties of simulated inertia-gravity and Rossby waves

3a. *Inertia-gravity waves*

The use of the optimal averaging in equations (5-7) results in the approximation of the frequency of inertia-gravity waves in the form:

$$\left(\frac{\nu}{f}\right)^2 = \mu^2 + 4\frac{\lambda^2}{d^2}\left(sin^2\frac{X}{2} + sin^2\frac{Y}{2}\right), \tag{21}$$

When the Rossby radius of deformation is well resolved by the grid resolution the C grid simulates well inertia-gravity waves. The optimal averaging of velocity components in the calculation of the Coriolis terms can only improve this result in comparison to that with the standard averaging scheme, because it should improve the simulated frequency of inertial oscillations without changing the simulated frequency of gravity waves. However, in this case the improvement will be

modest, because the result will be determined practically only by the simulated frequency of gravity waves. Therefore, we will not compare the result for the well resolved Rossby radius of deformation.

On the other hand, a number of studies (e.g. Wajsowicz 1986) showed that when the Rossby radius of deformation is not resolved well by the grid resolution the C grid inaccurately resolves the frequency of inertia-gravity waves. Figure 3 compares frequencies of inertia-gravity waves for a case when $r = (fd)^2/(4gH) = 2$. It also shows the B grid solution (e.g. Arakawa and Lamb 1977):

$$\left(\frac{\nu}{f}\right)^2 = 1 + 4\frac{\lambda^2}{d^2}\left(sin^2\frac{X}{2}cos^2\frac{Y}{2} + sin^2\frac{Y}{2}cos^2\frac{X}{2}\right). \tag{22}$$

[Figure 4 about here.]

Figure 3 shows that the inertia-gravity waves frequencies on the C grid with the standard averaging are always less than f, except for the longest wave, while in the analytical solution they are always grater than f. They are also descending with the increase of the wavenumber, for all wavelengths, while in the analytical solution they always increase. On the other hand, the optimal averaging in the Coriolis terms gives frequencies which for the long waves (waves longer than $4d$) are greater than f and monotonically grow with the increasing wavenumber. They

start to descend with the increasing wavenumber only for waves which are shorter than approximately $4d$ and become lower than f only for the shortest waves. It is important to notice that qualitatively the same improvement can be obtained also for larger values of r, because the choice of the optimization criteria results in the frequencies of inertial oscillations which are very close to the analytical solution for wavelengths greater or equal to $4d$ independently of r. We can also see that now for the long waves the result on the C grid is qualitatively similar to that obtained on the B grid.

A potential problem with the improved averaging on the C grid could be that, when the Rossby radius of deformation is not resolved well by the grid resolution, the group velocity is zero at the local maximum in inertia-gravity frequencies close to the point $(\pi/2, \pi/2)$ and at two saddle points close to $(\pi/2, 0)$ and $(0, \pi/2)$ (Figure 3). In the absence of the horizontal mixing and advection, it could happen that the energy at these particular wavenumbers wrongly accumulates. However, Figure 3 also shows that a similar problem exists on standard C and B grids, which have saddle points and zero group velocities at $(\pi/2, \pi/2)$. Therefore, we can assume that the energy accumulation problem should not significantly differ from that on the standard C grid. Numerical experiments in Section 4 will confirm this assumption. Another potential problem is that the averaging from

16 points requires additional boundary conditions for velocity components. The numerical experiment in Section 4 will also demonstrate that additional boundary conditions do not generate reflections.

3b. *Rossby waves*

Rossby waves can be isolated from the vorticity-divergence form of equations (1-2) in which we apply the β plane approximation ($\beta = \partial f/\partial y = const$):

$$\frac{\partial \zeta}{\partial t} + fD + \beta v = 0 \tag{23}$$

$$\frac{\partial D}{\partial t} - f\zeta + \beta u + g\nabla^2 h = 0, \tag{24}$$

where ζ is the vorticity and D is the divergence of the velocity. After combining equations (23-24) with equation (3) and neglecting small terms, we get:

$$\frac{\partial h}{\partial t} - \lambda^2 \nabla^2 \Big(\frac{\partial h}{\partial t} \Big) - \beta \lambda^2 \frac{\partial h}{\partial x} = 0. \tag{25}$$

The substitution of solutions in the form like (2) gives the frequency of Rossby waves:

$$\omega = \frac{-k\beta}{k^2 + l^2 + \lambda^{-2}}. \tag{26}$$

In order to obtain the finite difference approximation of equation (26) on the C grid with the optimized averaging in the Coriolis terms we will strictly follow the mathematical procedure from Wajsowicz (1986). The finite difference approximation of equations (1-2) will be:

$$\frac{\partial u}{\partial t} - \overline{f}^{oy}\overline{v}^{oxy} + g\delta_x h = 0 \tag{27}$$

$$\frac{\partial v}{\partial t} + f\overline{u}^{oxy} + g\delta_y h = 0. \tag{28}$$

The vorticity-divergence form of equations (23-24) in finite differences is:

$$\frac{\partial \zeta}{\partial t} + f\overline{D}^{oxy} + \beta\overline{\overline{v}^{oxy}}^{y} = 0 \tag{29}$$

$$\frac{\partial D}{\partial t} - \overline{f}^{oy}\overline{\zeta}^{oxy} + \beta\overline{\overline{u}^{oxy}}^{y} + g\nabla^2 h = 0. \tag{30}$$

The elimination of ζ and D from equations (29), (30) and (3), the neglecting of small terms, and noting that on he β plane $\overline{f}^{oy} = \overline{f}^{y} = f$, gives the finite difference approximation of equation (25):

$$\frac{\partial}{\partial t}\overline{\overline{h}^{oxy}}^{oxy} - \lambda^2\nabla^2\left(\frac{\partial h}{\partial t}\right) - \beta\lambda^2\delta_x\overline{\overline{h}^{oxy}}^{y} = 0. \tag{31}$$

The substitution of wave like solutions in the form like (2) into equation (31) gives the approximation of the frequency of Rossby waves in the form:

$$\omega = \frac{-\beta \frac{sin(X/2)cos(Y/2)}{(d/2)} \mu}{\frac{sin^2(X/2)}{(d/2)^2} + \frac{sin^2(Y/2)}{(d/2)^2} + \lambda^{-2}\mu^2}. \tag{32}$$

Now we will compare the properties of this approximation with the analytical solution of the Rossby wave frequencies given by equation (26), for 3 different values of $r = 0.1, 1, 10$. They correspond to grid resolutions which are finer, similar and coarser than the Rossby radius of deformation. We will also compare our solution with the approximations on the C grid with the standard averaging in the Coriolis terms and on the B grid computed by Wajsowicz (1986). The standard form on the C grid is:

$$\omega = \frac{-\beta \frac{sin(X)cos^2(Y/2)}{d}}{\frac{sin^2(X/2)}{(d/2)^2} + \frac{sin^2(Y/2)}{(d/2)^2} + \lambda^{-2}cos^2\frac{X}{2}cos^2\frac{Y}{2}}, \tag{33}$$

and the form on the B grid is:

$$\omega = \frac{-\beta \frac{sin(X)}{d}}{\frac{sin^2(X/2)cos^2(X/2)}{(d/2)^2} + \frac{sin^2(Y/2)cos^2(Y/2)}{(d/2)^2} + \lambda^{-2}}. \tag{34}$$

Figure 4 shows the analytical solution and finite differences approximations of

Rossby wave frequencies for $Y = 0$. We can see that the optimal averaging in the Coriolis terms on the C grid results in improved Rossby wave frequencies for long wavelengths. When $r = 0.1$, i.e. the when the grid resolution is much finer than the Rossby radius of deformation, it is generally accepted (e.g. Wajsowicz 1986; Neta and Williams 1989) that standard C and B grids simulate long Rossby waves in a satisfactory way and that the C grid is slightly more accurate for long waves. We can see in Figure 4 that the C grid with the optimal computation of the Coriolis term gives even more accurate frequencies for long waves. When $r = 10$, with the grid resolution coarser than the Rossby radius of deformation, the B grid is less accurate than the standard C grid, and the optimized averaging solution on the C grid again gives the most accurate solution for long wavelengths. However, unlike the analytical solution, all finite difference solutions give zero frequency for the shortest wavelength. A similar improvement for the simulation of frequencies of long waves was observed in the y direction in the two-dimensional graphs, but again the frequency of the shortest wave in the y direction was zero on all grids (not shown).

4. Numerical experiment

In order to demonstrate the improvement by the optimized averaging this section will present results of numerical experiments with the linear shallow water model defined on the C grid. Model equations are identical to those applied in Adcroft et al. (1999) and Nechaev and Yaremchuk (2004):

$$\frac{1}{\Delta t}\delta_t u - \overline{f\overline{v}^{x}}^{y} + \frac{g'}{d}\delta_x h = \frac{\tau_x}{\rho_0 H_0} - \epsilon u \tag{35}$$

$$\frac{1}{\Delta t}\delta_t v + \overline{f\overline{u}^{y}}^{x} + \frac{g'}{d}\delta_y h = -\epsilon v \tag{36}$$

$$\frac{1}{\Delta t}\delta_t h + \frac{H_0}{d}\Big(\delta_x u + \delta_y v\Big) = 0. \tag{37}$$

Also, most parameters of the model set-up are the same as in Adcroft et al. (1999). The model domain is defined on a flat bottom, square basin with depth $H_0 = 400m$ and length $L = 4000km$. The Coriolis parameter is $f = f_0 + \beta(y - L/2)$, where $f_0 = 10^{-4}s^{-1}$ and $\beta = 10^{-11}m^{-1}s^{-1}$. The reduced gravity is set to $g' = 10^{-2}m^2s^{-1}$ giving the Rossby radius of deformation $R = 20km$. The wind stress is specified in the form $\tau_x = \tau_0 sin[\pi(y - L/2)/L]$. Coriolis and pressure gradient terms are solved using the leap-frog scheme, and the bottom friction is solved using the Euler forward scheme. Time levels are filtered using the Asselin

time filter (Asselin 1972) with the filter parameter $c_A = 0.05$. The time step is $\Delta t = 1728s$. The averaging from 16 points in the Coriolis terms requires a boundary condition also for the velocity component parallel to the coast. It was set to zero on "land" points in order to ensure that boundary values do not change the energy.

This model set-up was chosen in order to make as similar as possible experiments to those in Adcroft et al. (1999). However, initial experiments with the same experimental set-up could not demonstrate the impact of the optimized averaging, because after initial time steps the relatively high bottom friction ($\epsilon = 10^{-6}s^{-1}$) damped all differences between low resolution experiments (not shown). Therefore, in order to demonstrate the impact of the improved averaging the bottom drag is set to $\epsilon = 10^{-8}s^{-1}$. This value significantly reduces the damping effect of the bottom friction and gives different experimental results at the low resolution. The model was integrated with $\tau_0 = 0.1Nm^{-2}$. Coarse resolution experiments were performed with the horizontal resolution $d = 100km$ ($r = 6.25$), and high resolution experiments with the horizontal resolution $d = 20km$ ($r = 0.25$).

[Figure 5 about here.]

Figure 5 shows surface height outputs for coarse and high resolution experiments after 3000 days of integration. The disturbance in the surface height field

propagates in the form of Rossby waves in the westward direction. With the high resolution (Figure 5d and 5e) the result is practically independent of α and is assumed to be the reference for low resolution experiments. At the low resolution the optimized averaging experiment (Figure 5b) gives a more accurate output than the standard averaging experiment (Figure 5a). In order to demonstrate that the higher accuracy of the output is due to the improved simulation of frequencies and not due to the slightly higher formal accuracy of the scheme, the same experiment is repeated with $\alpha = 1.08$. With this choice of α the absolute value of the truncation error is the same as with the optimal averaging, but the theoretical frequencies of long inertia-gravity and Rossby waves are more accurate than for the standard averaging ($\alpha = 1$) and less accurate than for $\alpha = 1.17$ (not shown). As a confirmation of the hypothesis that the accuracy of the simulated frequency creates the difference between low resolution experiments, Figure 5c shows that with $\alpha = 1.08$ the low resolution output has the intermediate accuracy.

In comparison to standard C grid outputs, and in agreement with the theoretical analysis from the previous section, optimized averaging outputs did not show any reflections at boundaries or the wrong energy accumulation. All experimental outputs had a relatively high level of small scale noise and were filtered for the presentation in Figure 5. However, optimized averaging outputs seemed

to produce more small scale noise at initial steps of the simulation (not shown). This experimental result is obtained with a linear model. We can expect that in a more realistic model, which includes the non-linear horizontal advection and the horizontal viscosity, the small scale noise will be attenuated.

5. Conclusions

We have theoretically demonstrated that the improved calculation of the Coriolis terms, by averaging from 16 surrounding points with optimally chosen weights, improves the simulation of long inertia-gravity and Rossby waves on the C grid, especially when the Rossby radius of deformation is not resolved well by the grid resolution. These theoretical findings were confirmed in numerical experiments with a linear shallow water model defined on the C grid. On the other hand, the theoretical analyses show that frequencies of the shortest waves remain poorly resolved, meaning that there remains the problem of the small scale noise when the grid resolution is much coarser than the Rossby radius of deformation. However, in realistic applications the shortest waves are anyway strongly dissipated by the scale selective horizontal viscosity commonly used in numerical models, and can be further attenuated by specially designed filters like those in Smith et al. (1990)

and Nechaev and Yaremchuk (2004). The optimized averaging facilitates the use of the scale selective filtering, because in comparison to the standard averaging its errors are more concentrated in short wavelengths.

We may expect that the optimized averaging could improve the simulation of long inertia-gravity and Rossby waves in the oceanographic models, when baroclinic Rossby radii of deformation are small in relation to the grid resolution. It can be easily incorporated into existing oceanographic models defined on the C grid, because it does not require any special time differencing scheme. Its computational requirement is practically negligible in comparison to the computational requirement of the whole model even with explicit methods for the temporal integration and small time steps. Therefore, the optimal averaging in the Coriolis terms could provide a computationally efficient alternative to the standard C grid averaging resulting in a more accurate simulation of long internal inertia-gravity and Rossby waves under a relatively large range of physical conditions.

Acknowledgments I would like to thank two unknown reviewers for their very helpful comments and suggestions. Financial support for my work was provided by EU projects MFSTEP (Mediterranean Forecasting System: Toward Environmental Prediction, Contract number: EVK3-CT-2002-00075) and MERSEA (Ma-

rine Environment and Security for the European Area, Contract number: SIP3-CT-2003-502885).

Appendix: Energy conserving form of the averaging from 16 points

The kinetic energy equation is formed by adding (19) multiplied by u to (20) multiplied by v. The energy conserving form of the optimized averaging requires that terms originating from Coriolis terms in (19) and (20) cancel when the energy equation is integrated horizontally. In order to demonstrate it we can use the property that the central averaging is the symmetric linear operator, which can be shown by integration by parts:

$$\sum_i a_i \overline{b}^{i^*} = \sum_i \overline{a}^{i+\frac{1}{2}^*} b_{i+1/2}, \tag{38}$$

and

$$\sum_i a_i \overline{b}^{i^{**}} = \sum_i \overline{a}^{i+\frac{1}{2}^{**}} b_{i+1/2}, \tag{39}$$

where the indexing corresponds to Figure 1. Therefore, the horizontal integration

of Coriolis terms in the kinetic energy equation gives:

$$\sum_{i,j}\left(\frac{u}{\Delta x}\overline{f\overline{V_{i+\frac{1}{2},j}}^{ox}}^{oy} - \frac{v}{\Delta y}\overline{f\overline{U_{i,j+\frac{1}{2}}}^{oy}}^{ox}\right)\Delta x\Delta y =$$

$$= \sum_{i,j} f\left(\overline{V_{i+\frac{1}{2},j+\frac{1}{2}}}^{ox}\overline{U_{i+\frac{1}{2},j+\frac{1}{2}}}^{oy} - \overline{U_{i+\frac{1}{2},j+\frac{1}{2}}}^{oy}\overline{V_{i+\frac{1}{2},j+\frac{1}{2}}}^{ox}\right) = 0. \qquad (40)$$

References

Adcroft, A.J., C.N. Hill, and J.C. Marshall (1999), A new treatment of the Coriolis terms in C-grid models at both high and low resolutions. *Mon. Wea. Rev., 127*, 1928-1936.

Arakawa, A., and V.R. Lamb (1977), Computational design of the basic dynamical processes of the UCLA general circulation model. *Methods in Computational Physics*, Ed. Chang J., Academic Press, 174-267.

Asselin, R. (1972), Frequency filter for time integrations. *Mon. Wea. Rev.*, *100*, 487-490.

Haidvogel, D.B., and A. Beckmann (1999), Numerical ocean circulation modeling. Imperial College Press, London, 320p.

Mesinger, F., and A. Arakawa (1976), Numerical methods used in atmospheric

models. Tech. Rep. WMO/ICSU Joint Organizing Comittee GARP Publ. Series.

Nechaev, D., and M. Yaremchuk (2004), On the approximation of the Coriolis term in C-grid models. *Mon. Wea. Rev.*, *132*, 2283-2289.

Neta, B., and R.T. Williams (1989), Rossby wave frequencies and group velocities for finite element and finite difference approximations to the vorticity-divergence and the primitive forms of the shallow water equations *Mon. Wea. Rev.*, *117*, 1439-1457.

Smith, R.D., D.B. Boudra, and R. Bleck (1990), A wind-driven isopycnal coordinate model of the north and equatorial Atlantic Ocean: The Atlantic-basin experiments. *J. Geophys. Res.*, *95*, 13105-13128.

Wajsowicz, R.C. (1986), Free planetary waves in finite-difference numerical models. *J. Phys. Ocean.*, *16*, 773-789.

List of Figures

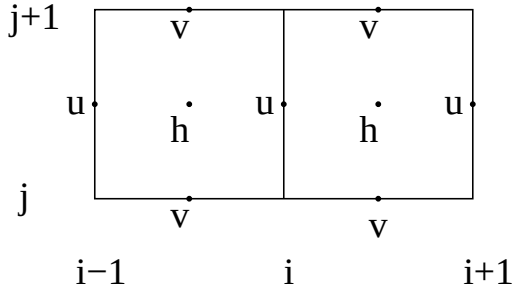

Figure 1: Distribution of computational points on the C grid.

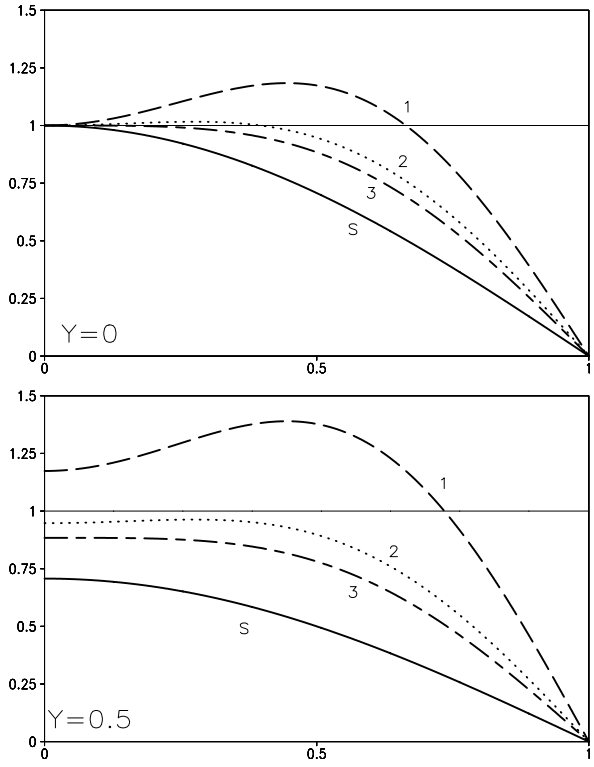

Figure 2: Frequencies of inertial oscillations scaled by f obtained for different values of the parameter α. The upper panel is for $Y = 0$, the lower panel is for $Y = \pi/2$, and the x axis is $x = X/\pi$. The continuous line (S) shows the standard averaging solution on the C grid ($\alpha = 1$). The long dashed line (1) shows the solution corresponding to $\alpha = 1.33$, the dotted line (2) the solution corresponding to $\alpha = 1.17$, and the long-short dashed line (3) the solution corresponding to $\alpha = 1.125$.

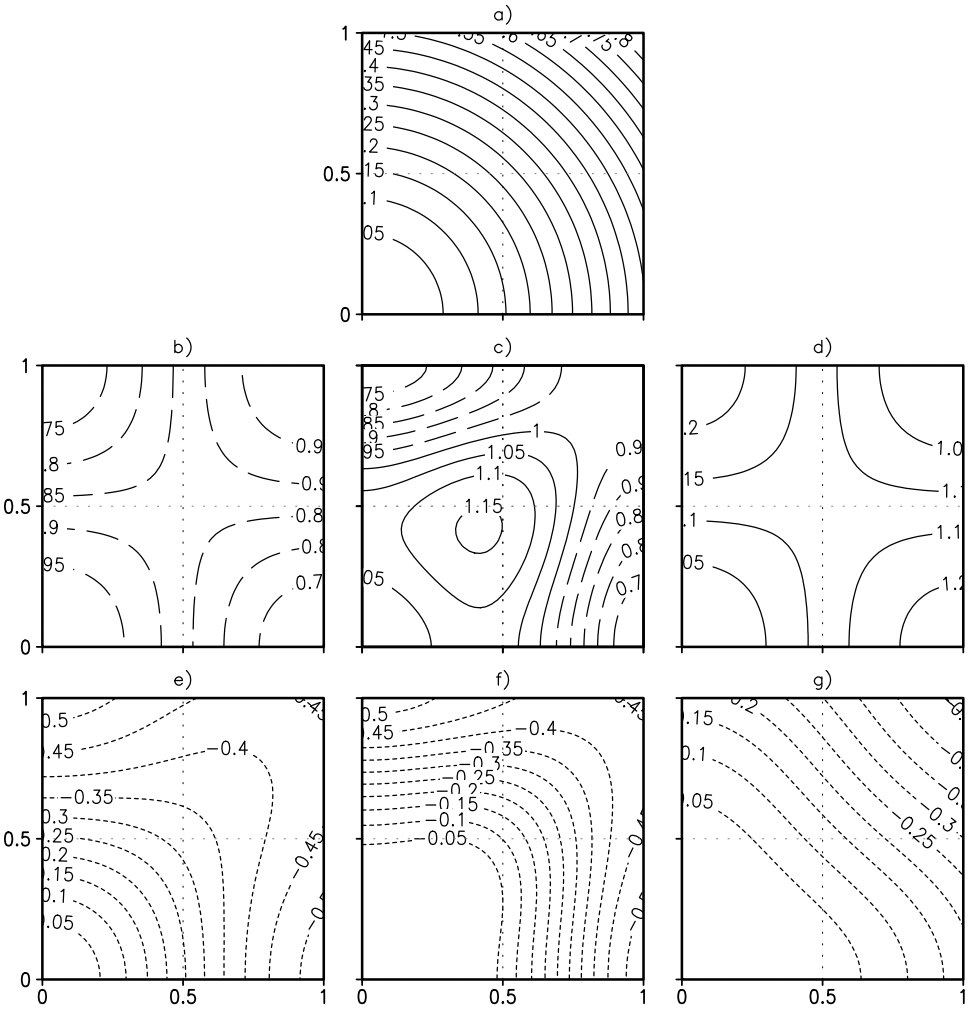

Figure 3: Frequencies of inertia-gravity waves scaled by f when $r = 2$. The x axis is $x = X/\pi$, and the y axis is $y = Y/\pi$. Long-dashed isolines are used for values less than 1. Due to the symmetry, the figure shows only the first quadrant. Panel a) shows analytical frequencies, panel b) the C grid frequencies with the standard averaging in the Coriolis terms, panel c) the C grid frequencies with the optimized averaging, and panel d) the B grid frequencies. Panels e), f) and g) correspond to frequencies in b), c) and d). They show relative errors of frequencies, i.e. $(\nu_c - \nu_a)/\nu_a$, where ν_c is the finite difference and ν_a the analytical frequency. Short-dashed lines are used for negative values.

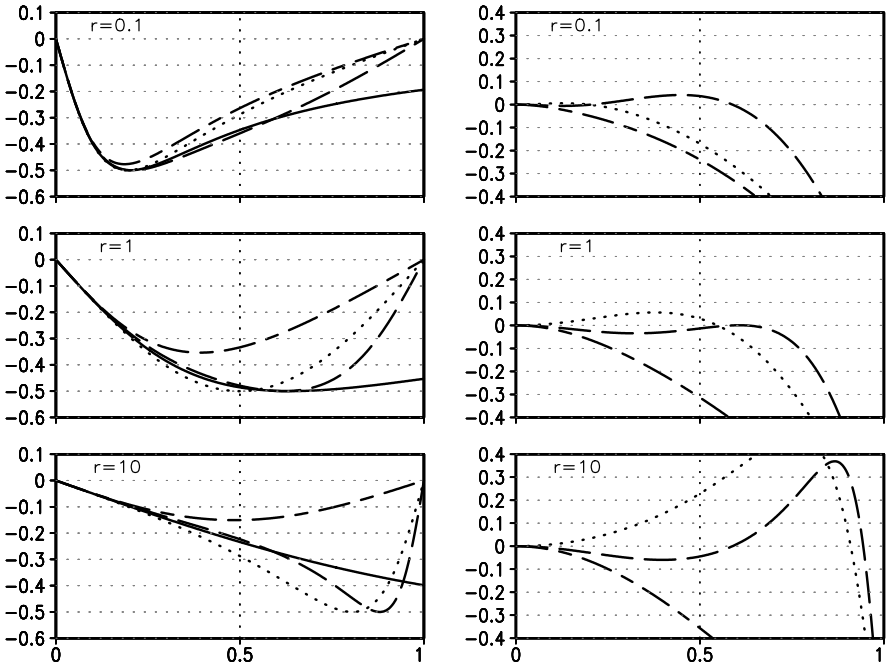

Figure 4: Frequencies of Rossby waves for $Y = 0$ in units of $\beta\lambda$ (left column) and their relative errors $(\omega_c - \omega_a)/\omega_a$ (right column), where ω_c is the finite difference and ω_a the analytical solution. Panels correspond to values of $r = 0.1, 1, 10$, and the x axis is $x = X/\pi$. The continuous line is the analytical solution, the dotted line is the standard C grid solution, the short-long dashed line is the B grid solution and the dashed line is the C grid solution with the optimal averaging in the Coriolis terms.

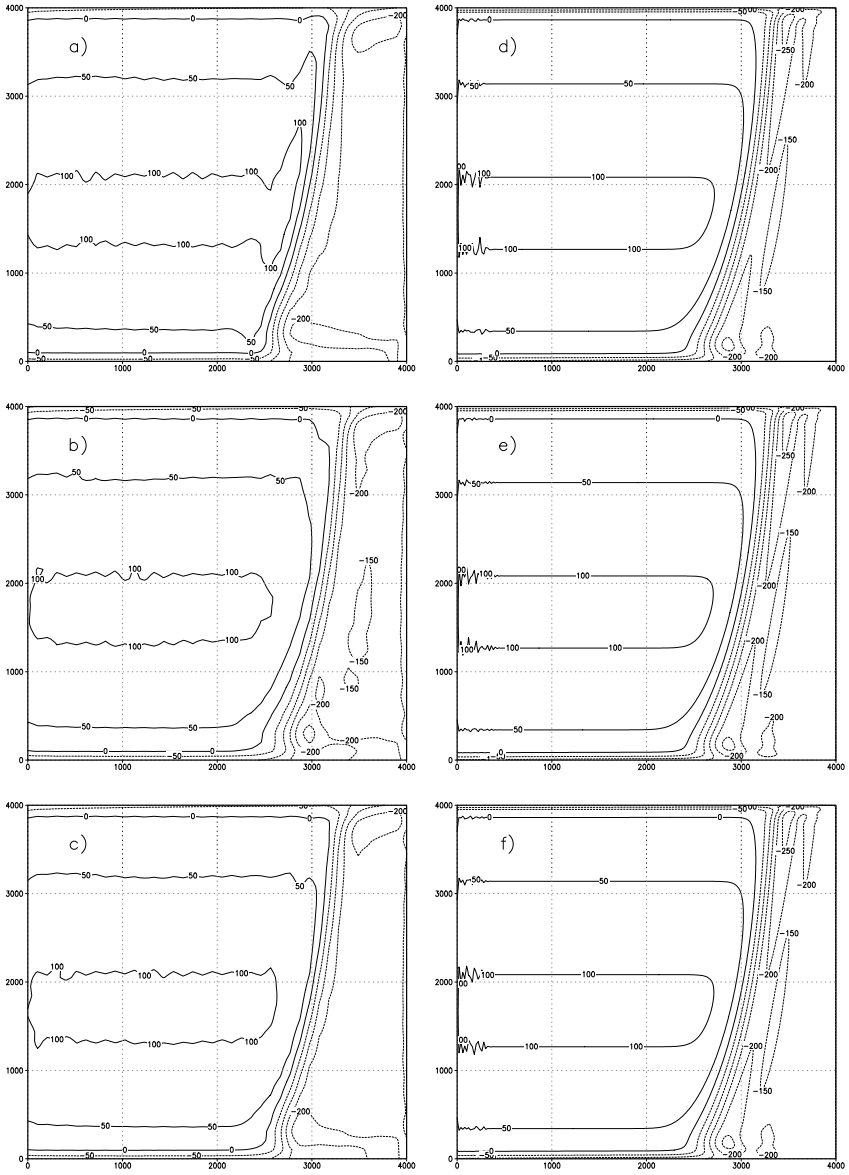

Figure 5: Surface height fields (m) after 3000 days of integration of the linear shallow water model. In order to present important features more clearly all fields are filtered with the 9 points filter. Panel a) represents result with the low resolution standard averaging ($\alpha = 1$), panel b) with the low resolution optimized averaging ($\alpha = 1.17$), and panel c) with the low resolution and $\alpha = 1.08$. Panels d), e) and f) are the same as a), b) and c), except for the high model resolution.